MCB
Journals.ASM.org

A Balance between Tel1 and Rif2 Activities Regulates Nucleolytic Processing and Elongation at Telomeres

Marina Martina, Michela Clerici, Veronica Baldo,* Diego Bonetti, Giovanna Lucchini, and Maria Pia Longhese

Dipartimento di Biotecnologie e Bioscienze, Università di Milano-Bicocca, Milan, Italy

Generation of G-strand overhangs at *Saccharomyces cerevisiae* yeast telomeres depends primarily on the MRX (Mre11-Rad50-Xrs2) complex, which is also necessary to maintain telomere length by recruiting the Tel1 kinase. MRX physically interacts with Rif2, which inhibits both resection and elongation of telomeres. We provide evidence that regulation of telomere processing and elongation relies on a balance between Tel1 and Rif2 activities. Tel1 regulates telomere nucleolytic processing by promoting MRX activity. In fact, the lack of Tel1 impairs MRX-dependent telomere resection, which is instead enhanced by the Tel1-hy909 mutant variant, which causes telomerase-dependent telomere overelongation. The Tel1-hy909 variant is more robustly associated than wild-type Tel1 to double-strand-break (DSB) ends carrying telomeric repeat sequences. Furthermore, it increases the persistence at a DSB adjacent to telomeric repeats of both MRX and Est1, which in turn likely account for the increased telomere resection and elongation in *TEL1-hy909* cells. Strikingly, Rif2 is unable to negatively regulate processing and lengthening at *TEL1-hy909* telomeres, indicating that the Tel1-hy909 variant overcomes the inhibitory activity exerted by Rif2 on MRX. Altogether, these findings highlight a primary role of Tel1 in overcoming Rif2-dependent negative regulation of MRX activity in telomere resection and elongation.

A highly ordered nucleoprotein complex called the telomere prevents the ends of linear chromosomes from being recognized as DNA double-strand breaks (DSBs) (reviewed in reference 30). Another key function of telomeres is to compensate for the incomplete replication of chromosome ends caused by discontinuous DNA synthesis. In most eukaryotes, telomeric DNA comprises tandemly repeated G-rich sequences (TG_{1-3} repeats in *Saccharomyces cerevisiae* yeast and T_2AG_3 in vertebrates), ending in a single-stranded 3′ overhang (G tail) (reviewed in reference 20). The addition of telomeric repeats depends on the action of telomerase, a specialized reverse transcriptase that extends the TG-rich strand of chromosome ends (23). The yeast telomerase complex consists of a reverse transcriptase subunit (Est2), a template RNA (TLC1), and two accessory proteins (Est1 and Est3), which are required for telomerase activity *in vivo* but not *in vitro*.

The single-stranded G tails of budding yeast telomeres are short (about 10 to 15 nucleotides [nt]) for most of the cell cycle, but their length increases transiently to 50 to 100 nucleotides in late S phase (15, 50). While telomeric G tails can be generated during lagging-strand replication by removal of the last RNA primer, the 5′ C strand of the telomere generated by leading-strand synthesis must be nucleolytically processed (resected) to generate 3′ overhangs (32, 51). Cyclin-dependent kinase (Cdk1 in *S. cerevisiae*) activity is required for this telomeric C-strand resection (17, 49), which occurs only during S and G_2 cell cycle phases, when Cdk1 activity is high and telomeres are elongated by telomerase (36). The MRX (Mre11-Rad50-Xrs2) complex and Sae2 have been shown to be important for resection of telomeric ends, with MRX playing the major role (8, 14, 28, 31). Moreover, Exo1 and Sgs1-Dna2 can provide a backup mechanism for telomere resection when Sae2-MRX activity is compromised (8).

In the yeast *Saccharomyces cerevisiae*, telomerase lengthens telomeres only in late S/G_2 phase (36). Although chromatin immunoprecipitation (ChIP) studies have found that Est2 is associated to telomeres from G_1 to late S phase (44), the use of live-cell imaging has shown that a subset of TLC1 molecules clusters and stably associates with telomeres only in late S phase (18). This clustering has been proposed to represent actively elongating telomeres (18), suggesting that regulation of telomerase activity is achieved at the level of its association with the telomere. In agreement with this hypothesis, budding yeast telomerase is preferentially enriched at short telomeres (4, 43), which are its preferred substrate (35, 45).

Telomere length maintenance depends on the checkpoint kinase Tel1, whose localization to chromosome ends requires the MRX complex (39). The function of Tel1 at telomeres relies on its kinase activity, since *tel1* kinase-dead cells have short telomeres like *tel1*Δ cells (22, 33). However, how Tel1 regulates telomere length is still unknown. Cells lacking Tel1 have a decreased frequency of telomerase-mediated telomere elongation (2). Furthermore, Tel1 has been shown to specifically associate with short telomeres (4, 25, 43) and is needed for preferential binding of Est1 and Est2 to them (21). These findings suggest that length-dependent binding of Tel1 to telomeres is a critical step in the regulation of telomerase association with telomeres in S phase. In budding yeast, telomerase recruitment at telomeres relies on a direct interaction between Est1 and the telomere end-binding protein Cdc13 (5, 9, 16, 40). It has been proposed that Tel1 promotes Est1-Cdc13 interaction by phosphorylating the telomerase recruitment domain of Cdc13 (46), although this model has recently been ques-

Received 8 November 2011 **Returned for modification** 13 December 2011
Accepted 10 February 2012
Published ahead of print 21 February 2012

Address correspondence to Maria Pia Longhese, mariapia.longhese@unimib.it.
* Present address: Ludwig Institute for Cancer Research, University of California, San Diego, La Jolla, California, USA.

Supplemental material for this article may be found at http://mcb.asm.org/.

doi:10.1128/MCB.06547-11

tioned (19). Tel1 is also important for increasing telomerase processivity at critically short telomeres (10). However, since the occurrence of critically short telomeres (<125 bp in length) should be relatively infrequent, the primary cause of the short *tel1*Δ telomeres has been proposed to be a reduced frequency of elongation by telomerase, rather than a reduced telomerase processivity (10).

The identity of *S. cerevisiae* telomeres also relies on a protein complex formed by the Rap1, Rif1, and Rif2 proteins, which inhibit telomerase-dependent telomere elongation (12, 24, 29, 52). Rif2 physically interacts with MRX *in vitro* (26) and inhibits MRX-dependent 5′-end resection at telomeres (6, 7). Furthermore, the lack of Rif2 enhances MRX and Tel1 association at telomeres (7, 26), suggesting that Rif2 regulates nucleolytic processing of telomeres by inhibiting MRX recruitment. However, the artificial tethering of Rif2 at DNA ends leads to decreased Tel1 binding, but not MRX binding, to these ends (26), indicating that Rif2 counteracts Tel1 association to DNA ends. This observation, together with the finding that MRX localization at telomeres is reduced in *tel1*Δ cells compared to wild-type cells (26), raises the possibility that Tel1, after its MRX-dependent loading onto telomeric ends, can enhance MRX activity. As MRX is required to generate telomeric single-stranded DNA (ssDNA), this Tel1-dependent regulation of MRX might influence resection of telomeric ends. Consistent with this hypothesis, loss of Tel1 in telomerase-negative cells attenuates the onset of senescence (19, 42), whose primary signal has been proposed to be telomeric ssDNA (1).

To study the physiological consequences of the Tel1-mediated feedback loop on MRX, as well as the role of Rif2 in counteracting Tel1/MRX function, we took advantage of the *TEL1-hy909* mutant allele, previously identified to be a dominant suppressor of the hypersensitivity to genotoxic agents and checkpoint defects of Mec1-deficient cells (3). Here we provide evidence that Tel1 regulates G-tail generation at telomeres by promoting MRX function. In fact, the lack of Tel1 impairs MRX-dependent generation of ssDNA at telomeres, whereas the Tel1-hy909 variant enhances both resection and elongation of telomeric ends. Moreover, Tel1-hy909 is more robustly associated to DSBs adjacent to telomeric tracts than wild-type Tel1 and also enhances MRX and Est1 binding at these DNA ends. These findings, together with the observation that *TEL1-hy909* telomeres escape the negative regulation exerted by Rif2 on both processing and elongation, indicate that Rif2-mediated inhibition of Tel1/MRX activity is important to regulate nucleolytic processing and elongation of telomeres.

MATERIALS AND METHODS

Strains. Strain genotypes are listed in Table S1 in the supplemental material. The strains used for monitoring resection at the HO-induced DSB adjacent to telomeric repeats were derivatives of strain UCC5913, kindly provided by D. Gottschling (Fred Hutchinson Cancer Research Center, Seattle, WA). The strains used for monitoring resection at the HO-induced DSB were derivatives of strain RMY169, kindly provided by T. Weinert (University of Arizona, Tucson, AZ), and JKM139, kindly provided by J. Haber (Brandeis University, Waltham, MA). Strain RMY169 was created by replacing the *ADE2-TG* cassette of strain UCC5913 with the *TRP1* gene (38). The strains used for monitoring telomere addition at an HO-induced DSB adjacent to telomeric repeats were derivatives of strain YSN645, kindly provided by D. Shore (University of Geneva, Geneva, Switzerland). Strains UCC5913, RMY169, YSN645, and JKM139 were used to replace the *TEL1* chromosomal copy with the *TEL1-hy909* allele by PCR, giving rise to strains YLL2836, YLL3066, YLL2255, and YLL2880, respectively. To induce a persistent G_1 arrest with α-factor, the *BAR1* gene, which encodes a protease that degrades the α-factor, was deleted. Deletions of the *YKU70*, *EXO1*, *MRE11*, *TEL1*, *RIF1*, *RIF2*, *RAD51*, *RAD52*, *EST2*, and *BAR1* genes were generated by a one-step PCR disruption method. A *TEL1-hy909 xrs2-11* strain was obtained by crossing strain KSC1563 (*MAT***a**-*inc ADH4cs*::*HIS2 ade1 his2 leu2 trp1 ura3 xrs2-11*::*KANMX4 sml1*::*LEU2*), kindly provided by K. Sugimoto (University of New Jersey, Newark, NJ), with a *TEL1-hy909* strain. Strain YLL3068, carrying a fully functional *TEL1-HA* allele at the *TEL1* chromosomal locus (the hemagglutinin [HA] tag coding sequence was located 2,394 bp downstream of the *TEL1* start codon), was obtained by transforming strain YLL2599 with a PCR product obtained using genomic DNA of strain YLL3001 as the template together with primers PRP1297 (5′-GGC CAC CGT TAA GAA GGG TAA GCC AGA A-3′) and PRP1298 (5′-GTT GCA AAG ACT CTC TGC TTC CCA CCT C-3′). Strain YLL3001 was a derivative of strain KRY22, kindly provided by T. Petes (Duke University School of Medicine, Durham, NC), in which the *NATMX* cassette was inserted upstream of the *TEL1* start codon. Strain YLL3003, carrying the HA-tagged *TEL1-hy909* allele at the *TEL1* chromosomal locus, was obtained by transforming strain YLL2836 with a PCR product obtained using genomic DNA of strain YLL3001 as the template together with primers PRP1297 and PRP1298. PCR one-step tagging was used to obtain strains carrying fully functional MYC-tagged *MRE11* and MYC-tagged *EST1* alleles. The *TEL1-hy909kd* allele, encoding a kinase-defective Tel1-hy909 variant carrying the amino acid changes G2611D, D2612A, N2616K, and D2631E, was obtained by site-directed mutagenesis. The accuracy of all gene replacements and integrations was verified by Southern blot analysis or PCR. Cells were grown in YEP medium (1% yeast extract, 2% Bacto peptone, 50 mg/liter adenine) supplemented with 2% glucose (YEPD) or 3% glycerol, 2% lactic acid, and 0.05% glucose or with 3% glycerol, 2% lactic acid, and 2% galactose.

Resection assay. Visualization of the single-stranded overhangs at native telomeres was done as described previously (15). The same gel was denatured and hybridized with the end-labeled C-rich oligonucleotide for loading control. Resection of the 5′ strand at the HO-induced DSB adjacent to telomeric repeat sequences was monitored as previously described (7). To monitor resection at the HO-induced DSB, SspI- and XbaI-digested genomic DNA was hybridized with a single-stranded riboprobe, which anneals to the 5′ strand to a site located 248 nt from the HO cutting site. For quantitative analysis of resection, the ratios between the intensities of the cut 5′ strand and loading control bands were calculated by using the NIH image program. For quantitative analysis of G-tail signals at native telomeres, the ratios between the intensities of the TG-ssDNA signals on the native gels and the total amount of TG repeats revealed by the same probe after denaturation of the gels were calculated by using the NIH image program.

ChIP analysis. ChIP analysis was performed as previously described (47). After exposure to formaldehyde, chromatin samples were immunoprecipitated with appropriate antibodies. Quantification of immunoprecipitated DNA was achieved by quantitative real-time PCR (qPCR) on a Bio-Rad MiniOpticon apparatus using primer pairs located at the nontelomeric *ARO1* fragment of chromosome IV (CON) and 640 bp centromere proximal (TG-HO) or 550 bp centromere distal (HO) to the HO cutting site at chromosome VII, and the amount was normalized to the input signal for each primer set; data are expressed as the fold enrichment of TG-HO or HO over the amount of CON in the immunoprecipitates.

RESULTS

Tel1-hy909 causes MRX- and telomerase-dependent telomere overelongation. In a screening for *TEL1* mutations that suppressed the hypersensitivity to genotoxic agents of *mec1*Δ cells, we previously identified 7 *TEL1-hy* alleles which can partially bypass the Mec1 requirement for checkpoint activation (3). Most of the Tel1-hy variants displayed enhanced kinase activity *in vitro* com-

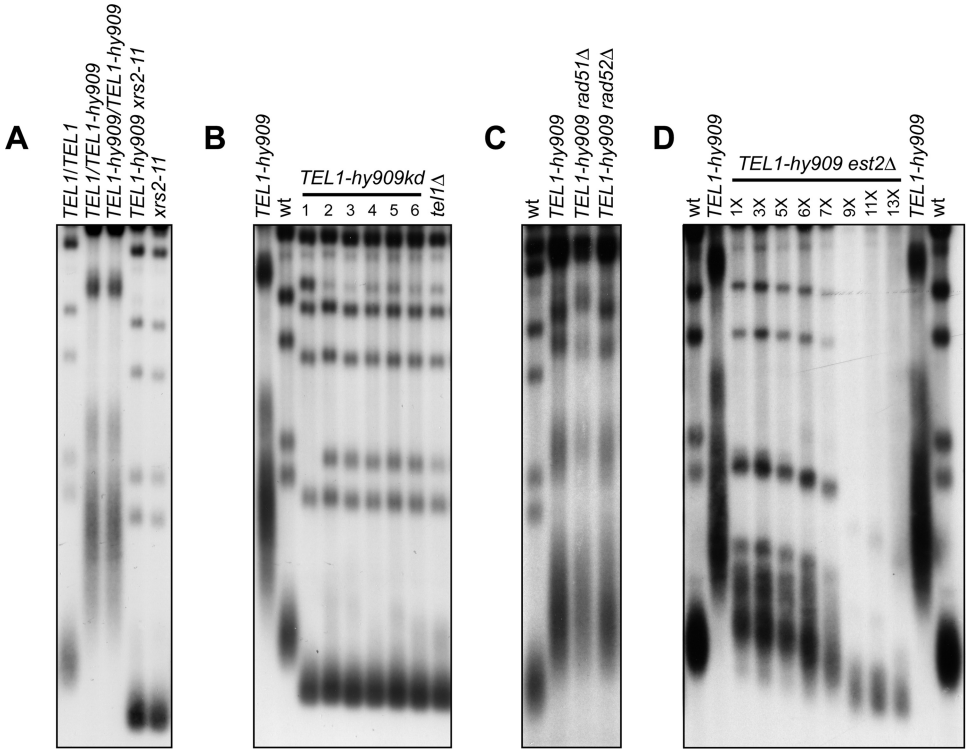

FIG 1 Telomere overelongation in *TEL1-hy909* cells. (A to C) XhoI-cut genomic DNA from exponentially growing cells (YEPD at 25°C) was subjected to Southern blot analysis using a radiolabeled poly(GT) telomere-specific probe. For panel B, 6 independent *TEL1-hy909kd* transformant clones were analyzed (lanes 1 to 6). (D) Meiotic tetrads from *EST2*/*est2*Δ *TEL1*/*TEL1-hy909* diploid cells were dissected on YEPD plates. After ~25 generations, *TEL1-hy909 est2*Δ spore clones were streaked for successive times (1 to 13 times) and aliquots of cells from the indicated streaks were propagated in YEPD liquid medium for 5 h to prepare genomic DNA for telomere length detection, as in panels A to C. Each subsequent streak represents ~25 generations of growth. wt, wild type.

pared to wild-type Tel1, but only the Tel1-hy909 variant causes an impressive telomere elongation (3) (Fig. 1).

The overelongated telomere phenotype of *TEL1-hy909* cells is dominant and requires Tel1 kinase activity. In fact, *TEL1-hy909* heterozygous and homozygous diploid cells exhibited very similar telomere lengths (Fig. 1A). Furthermore, cells expressing a Tel1-hy909 variant carrying the G2611D, D2612A, N2616K, and D2631E amino acid changes (Tel1-hy909kd in Fig. 1B), which were shown to destroy Tel1 kinase activity (33), had telomeres as short as those of *tel1*Δ cells (Fig. 1B). These data further support previous findings that Tel1 acts as a kinase to maintain telomere length (33).

The MRX complex is required to load Tel1 onto DNA ends (39). MRX is properly assembled and binds DSBs in *xrs2-11* cells, which express truncated Xrs2 lacking the C-terminal 162 amino acids, but Tel1 binding to DSBs is compromised in the same cells (39). As shown in Fig. 1A, telomeres in *xrs2-11 TEL1-hy909* double mutant cells were as short as in *xrs2-11* single mutant cells, indicating that Tel1-hy909 action at telomeres does not bypass MRX requirement.

Telomere elongation is primarily accomplished by telomerase and occasionally by homologous recombination, but the latter does not seem to have a role in Tel1-hy909-induced telomere overelongation. In fact, the lack of the recombination protein Rad51 or Rad52 in *TEL1-hy909* cells did not modify telomere length (Fig. 1C). We then assessed the contribution of the telomerase enzyme to this *TEL1-hy909* phenotype by dissecting meiotic tetrads from a diploid strain heterozygous for the *est2*Δ and *TEL1-hy909* alleles. After 2 days of incubation at 25°C (approximately 25 generations), spore clones were streaked for successive times, and aliquots of cells from the indicated streaks were propagated in YEPD liquid medium for 5 h to prepare genomic DNA for telomere length analysis (Fig. 1D). Telomeres underwent progressive shortening in *TEL1-hy909 est2*Δ clones (Fig. 1D), indicating that *TEL1-hy909*-dependent telomere overelongation requires telomerase activity.

The *tel1*Δ and *TEL1-hy909* mutations exert opposite effects on ssDNA generation at a DSB adjacent to telomeric repeat sequences. Because the absence of Tel1 attenuates the senescence phenotype of telomerase-negative cells, it was suggested that Tel1 has additional functions at telomeres besides directly affecting telomerase action (19, 42). Tel1 recruitment at telomeres requires the MRX complex (39), which is necessary to generate 3′-ended ssDNA at telomeric ends (8, 14, 28). MRX association to telomeres is decreased in *tel1*Δ cells (26), suggesting that Tel1 may be involved in stimulating resection of the telomeric ends by promoting MRX activity. To assess whether Tel1 exerts a positive-feedback loop on MRX *in vivo*, we analyzed resection of telomeric ends in *tel1*Δ and *TEL1-hy909* cells. We used an assay initially developed to examine *de novo* telomere formation (13, 14), where an 81-bp TG repeat sequence is placed immediately adjacent to an HO endonuclease cut site (Fig. 2A). The strain carries this HO cleavage site inserted into the *ADH4* locus on chromosome VII and expresses the HO endonuclease gene from a galactose-inducible promoter. Upon cleavage by HO, the centromere-proximal TG side of the break is "healed" by telomerase and gives rise to a

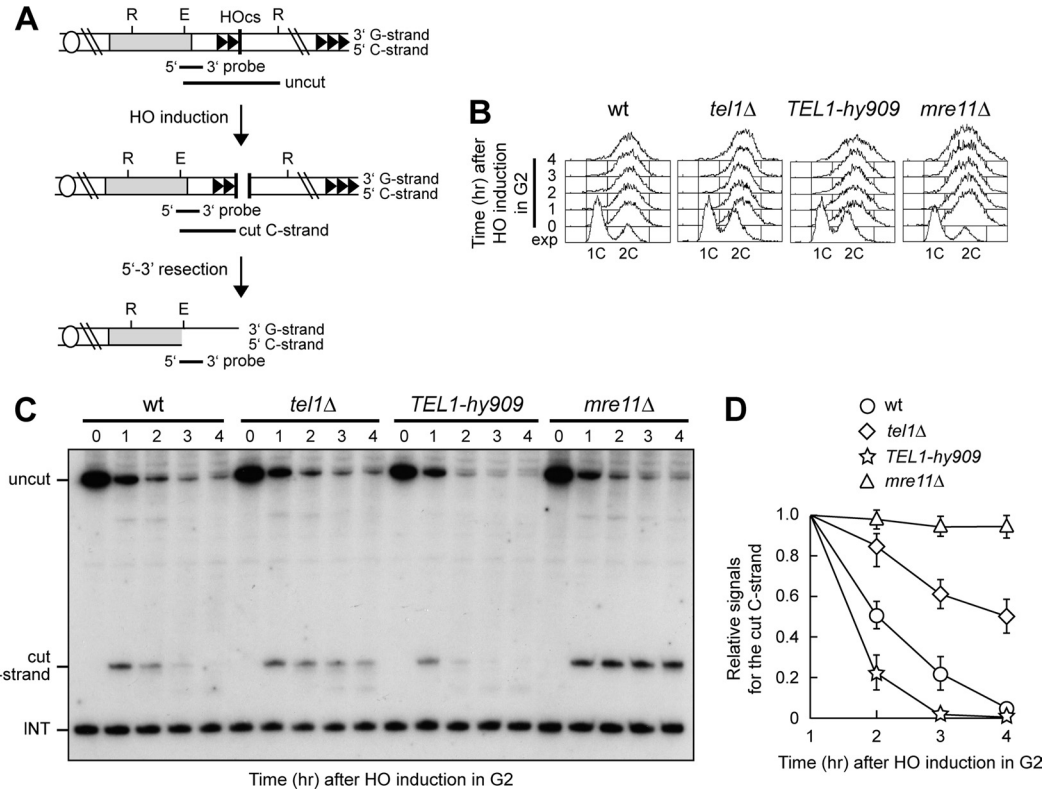

FIG 2 Effects of the *tel1*Δ and *TEL1-hy909* mutations on ssDNA generation at a DSB end carrying telomeric repeats. (A) Schematic representation of the HO cleavage site (HOcs) with the TG repeat sequences (81 bp; two arrowheads) that were placed centromere proximal to the HO site at the *ADH4* locus on chromosome VII-L. The centromere is shown as a circle on the left. The probe used to monitor nucleolytic degradation of the 5′ C strand is also indicated. R, RsaI; E, EcoRV. (B to D) HO expression was induced at time zero by galactose addition to nocodazole-arrested cell cultures that were kept arrested in G_2. (B) Fluorescence-activated cell sorter analysis of DNA content. exp, exponentially growing cells. (C) RsaI- and EcoRV-digested genomic DNA was hybridized with a single-stranded riboprobe that anneals to the 5′ C strand to a site located 212 bp from the HO cutting site. The probe reveals an uncut 390-nt DNA fragment (uncut), which is converted by HO cleavage into a 166-nt fragment (cut C strand). Degradation of the 5′ C strand leads to disappearance of the probe signal as resection proceeds beyond the hybridization region. The probe also detects a 138-nt fragment from the *ade2-101* locus on chromosome XV (INT), which serves as internal loading control. (D) Densitometric analysis. Plotted values are means ± SDs from three independent experiments, as in panel C.

bona fide telomere (13, 14). DNA degradation was assessed by Southern blotting under denaturing conditions using a single-stranded riboprobe that recognizes the 5′ C strand (Fig. 2A). Upon digestion of genomic DNA with EcoRV and RsaI restriction enzymes, the probe reveals an uncut 390-nt DNA fragment (uncut), which is converted by HO cleavage into a 166-nt fragment (cut C strand) (Fig. 2A). Degradation of the 5′ C strand leads to disappearance of the probe signal when resection proceeds beyond the hybridization region.

As generation of ssDNA at telomeres occurs during S and G_2/M cell cycle phases, when Cdk1 activity is high (17, 49), we monitored 5′-3′ resection of the TG DSB end by inducing HO expression in *tel1*Δ, *TEL1-hy909*, and *mre11*Δ cells that were kept arrested in G_2 with nocodazole (Fig. 2B). Degradation of the band corresponding to the cut 5′ C strand (cut C strand) occurred more slowly in G_2-arrested *tel1*Δ cells than in wild type, and it was completely abolished, as expected (14, 28), in G_2-arrested *mre11*Δ cells (Fig. 2C and D). In contrast, 5′ C-strand degradation was more efficient in *TEL1-hy909* cells than in wild type (Fig. 2C and D). Thus, the lack of Tel1 impairs resection at DSB ends adjacent to telomeric DNA, while Tel1-hy909 increases its efficiency. These observations, together with the notion that 5′ C-strand degradation in G_2-arrested cells requires the MRX complex (Fig. 2C and D) (14, 28), indicate that Tel1 influences 5′-3′ nucleolytic processing of these DNA ends by promoting MRX activity. Interestingly, MRX function is not completely abrogated by the lack of Tel1, as 5′ C-strand degradation in *tel1*Δ cells was reduced but not completely abolished as it was in *mre11*Δ cells (Fig. 2C and D).

The Tel1-hy909 variant might enhance nucleolytic processing at telomeres by hyperactivating the MRX complex. As nucleolytic degradation at telomeres requires Cdk1 activity (17, 49), which is thought to activate the MRX-dependent resection machinery (6, 7), we asked whether the Tel1-hy909 variant bypasses Cdk1 requirement for resection of a DSB adjacent to telomeric repeat sequences. To this end, the HO cut was induced in G_1-arrested wild-type and *TEL1-hy909* cells (Fig. 3A) carrying the system described in Fig. 2A. Consistent with the requirement of Cdk1 activity for DNA end resection, the 5′ C-rich strand signal was stable in G_1-arrested wild-type cells (Fig. 3B and C). In contrast, it progressively decreased in G_1-arrested *TEL1-hy909* cells (Fig. 3B and C), indicating that the *TEL1-hy909* mutation allows Cdk1-independent nucleolytic processing of a DSB end with telomeric repeats. This ability of Tel1-hy909 to bypass Cdk1 requirement for resection depends on Tel1 kinase activity, as 5′ C-strand degradation was prevented in G_1-arrested *TEL1-hy909kd* cells (Fig. 3A to C). Furthermore, this Tel1-hy909-dependent resection specifically re-

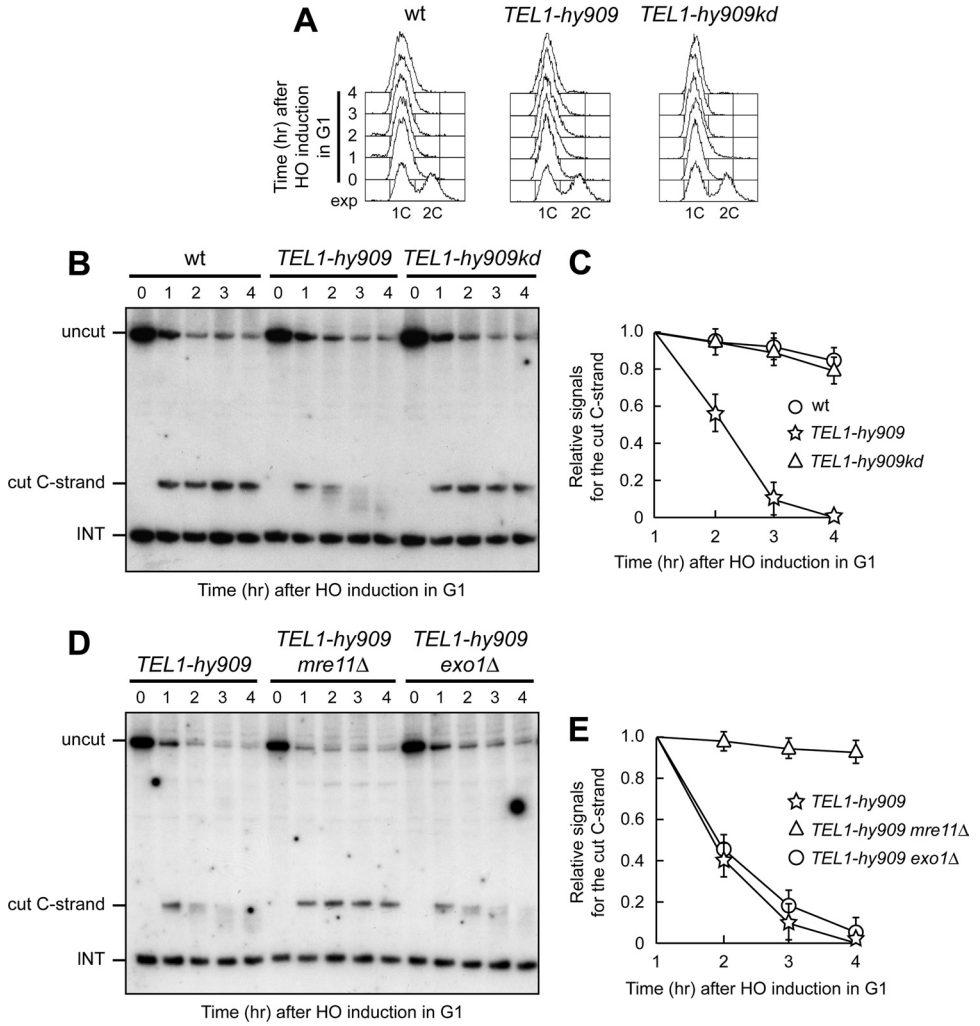

FIG 3 Tel1-hy909 allows resection in G_1 of a DSB adjacent to telomeric repeats. (A to C) HO expression was induced at time zero by galactose addition to α-factor-arrested cells, all carrying the system described in Fig. 2A. Cells were kept arrested in G_1. (A) Fluorescence-activated cell sorter analysis of DNA content. (B) RsaI- and EcoRV-digested genomic DNA was analyzed as described in the legend to Fig. 2C. (C) Densitometric analysis. Plotted values are means ± SDs from three independent experiments, as in panel B. (D and E) HO expression was induced at time zero by galactose addition to α-factor-arrested cells that were kept arrested in G_1. Cell cycle arrest was verified by fluorescence-activated cell sorter analysis (data not shown). (D) RsaI- and EcoRV-digested genomic DNA was analyzed as described in the legend to Fig. 2C. (E) Densitometric analysis. Plotted values are means ± SDs from three independent experiments, as in panel D.

quires MRX, because it was abolished in G_1-arrested *TEL1-hy909 mre11*Δ cells, whereas it took place in *TEL1-hy909* cells lacking the Exo1 nuclease (Fig. 3D and E). As Cdk1 has been proposed to induce DSB resection by increasing the efficiency of the MRX-dependent resection machinery (6, 7), these data are consistent with the hypothesis that Tel1-hy909 hyperactivates MRX.

Tel1-hy909 does not bypass Cdk1 requirement to generate ssDNA at DSB ends lacking telomeric repeats. We have previously shown that Tel1-hy909 increases ssDNA generation at intrachromosomal DSBs in G_2-arrested cells (3). Thus, we asked whether the Tel1-hy909 variant could bypass Cdk1 requirement for ssDNA generation at an HO-induced DSB devoid of telomeric repeats, as it does when the DSB is adjacent to telomeric tracts (Fig. 3). HO expression was induced in G_1-arrested wild-type and *TEL1-hy909* cell cultures that carried an HO cut site with no TG repeats (Fig. 4A) and that were kept arrested in G_1 with α-factor (Fig. 4B). In contrast to what happens at a DSB end carrying telomeric repeats, whose resection was completely abolished in G_1 (Fig. 3B and C), a degradation of the 5′ DSB end with no TG repeats still occurred in G_1-arrested wild-type cells (Fig. 4C and D), although it was less efficient than that detected at the same DSB in G_2 (data not shown) (27). On the other hand, *TEL1-hy909* G_1 cells showed a behavior very similar to that of wild type (Fig. 4C and D), indicating that Tel1-hy909 does not promote Cdk1-independent 5′-3′ nucleolytic processing at DSB ends that do not carry telomeric DNA sequences. This hypothesis was further confirmed by the observation that both wild-type and *TEL1-hy909* G_1 cells generated very similar small amounts of 3′-ended single-stranded resection products at an irreparable HO-induced DSB generated at the *MAT* locus (see Fig. S1 in the supplemental material). Thus, we can conclude that Tel1-hy909 in G_1 exerts its action preferentially at DNA ends adjacent to telomeric repeat sequences.

The *tel1*Δ and *TEL1-hy909* mutations exert opposite effects at native telomeres. The above-described findings prompted us to

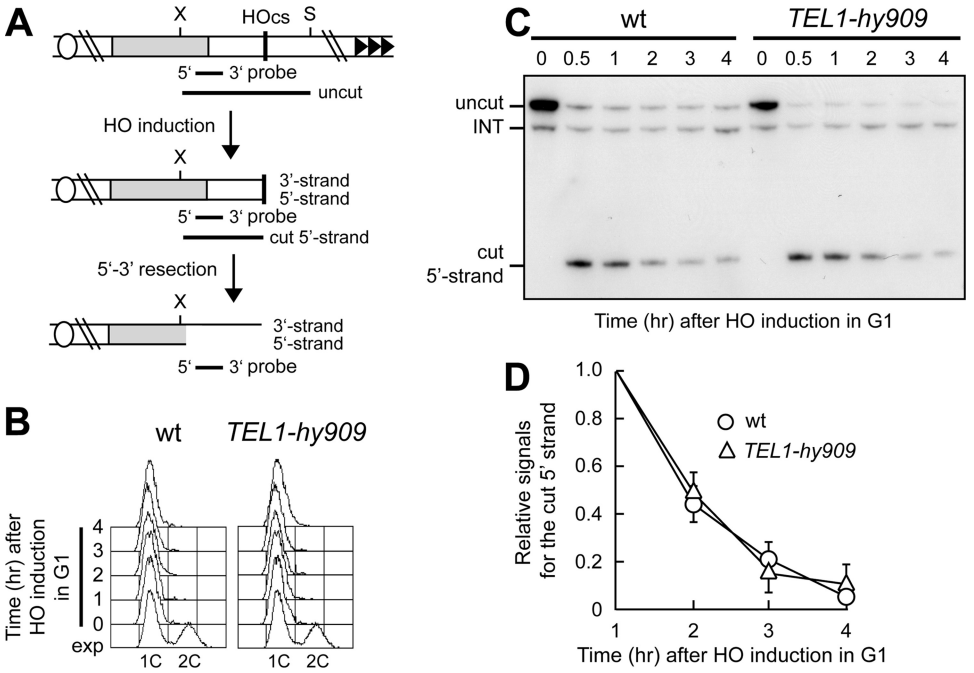

FIG 4 Tel1-hy909 does not enhance nucleolytic processing in G_1 of a DSB with no telomeric repeats. (A) Schematic representation of the system used to generate the HO-induced DSB on chromosome VII. SspI- and XbaI-digested genomic DNA is hybridized with the indicated single-stranded probe that anneals to the 5′ strand to a site located 248 nt from the HO cutting site, revealing an uncut 897-nt DNA fragment (uncut), which is converted by HO cleavage into a 286-nt fragment (cut 5′ strand). Loss of the 5′ strand beyond the hybridization region of the probe leads to disappearance of the signal generated by the probe. S, SspI; X, XbaI. (B to D) HO expression was induced at time zero by galactose addition to α-factor-arrested wild-type and *TEL1-hy909* cells, all carrying the system depicted in panel A. Cells were kept arrested in G_1. (B) Fluorescence-activated cell sorter analysis of DNA content. (C) SspI- and XbaI-digested genomic DNA was hybridized with the probe described in panel A. (D) Densitometric analysis. Plotted values are means ± SDs from four independent experiments, as in panel C.

investigate whether the role of Tel1 in promoting ssDNA generation at DSB ends carrying TG repeats could be extended to native telomeres. To assess the presence of ssDNA at natural chromosome ends, genomic DNA prepared from exponentially growing cells was analyzed by nondenaturing in-gel hybridization with a C-rich radiolabeled oligonucleotide that detect the G-rich single-stranded telomere overhangs (15). Because *tel1*Δ telomeres have fewer TG sequences than wild-type telomeres, the TG-ssDNA signals were normalized to the total amount of TG repeats revealed by the same probe after denaturation of the gel. Consistent with a role of Tel1 in promoting single-stranded overhang generation also at native chromosome ends, the amount of ssDNA was lower at *tel1*Δ telomeres than at wild-type telomeres (Fig. 5A and B). As previously observed (14, 28), *mre11*Δ telomeres also displayed a reduced amount of telomeric ssDNA compared to wild type (Fig. 5A and B). However, similar to what happens at the DSB ends carrying telomeric repeats (Fig. 2C and D), the single-stranded G-tail signal was lower in *mre11*Δ than in *tel1*Δ cells (Fig. 5A and B), indicating that MRX activity at telomeres is not completely abolished by the lack of Tel1.

The same analysis showed a stronger intensity of the G-tail signal in exponentially growing *TEL1-hy909* cells than in wild-type cells (Fig. 5A and B). The ssDNA formation at *TEL1-hy909* telomeres depends on the MRX complex, as the lack of Mre11 reduced the amount of the G-tail signal in *TEL1-hy909* cells to the level observed in *mre11*Δ cells (Fig. 5A and B). Furthermore, the strong ssDNA signal at *TEL1-hy909* telomeres was due to resection rather than to telomerase action, because similar amounts of telomeric ssDNA were detected during successive streaks of *TEL1-hy909* cells that shortened telomeres due to the absence of the telomerase subunit Est2 (Fig. 5C and D).

The Tel1-hy909 variant allows resection of a DSB end with telomeric repeats even in G_1 (Fig. 3), and this property is extended to native telomeres. In fact, when *TEL1-hy909* cells were arrested in G_1 with α-factor and released into the cell cycle (Fig. 5E), the intensity of the telomeric ssDNA signal in G_1-arrested cells was similar to that observed both during exponential growth and at different times after release (Fig. 5F and G). Thus, the Tel1-hy909 variant appears to bypass Cdk1 requirement for ssDNA generation even at native telomeres.

Because ssDNA at telomeres has been proposed to signal the onset of senescence (1), we could expect differences in the decline of growth of *est2*Δ versus *est2*Δ *TEL1-hy909* cells. Meiotic tetrads were dissected from a diploid strain heterozygous for both *est2*Δ and *TEL1-hy909*. After incubation for 2 days at 25°C (approximately 25 generations), spore clones were streaked for successive times (Fig. 6A) and an aliquot of cells from each streak was propagated in YEPD liquid medium for 5 h to prepare genomic DNA for telomere length analysis (Fig. 6B). As the *TEL1-hy909* allele also causes telomere overelongation under heterozygous conditions (Fig. 1A), *est2*Δ and *est2*Δ *TEL1-hy909* spores started with similar very long telomeres, which shortened during the subsequent subculturings (Fig. 6B). Consistent with the enhanced resection promoted by Tel1-hy909, the telomeres shortened slightly faster in *est2*Δ *TEL1-hy909* than in *est2*Δ cells (Fig. 6B). Furthermore, *TEL1-hy909 est2*Δ cells showed a senescent phenotype at

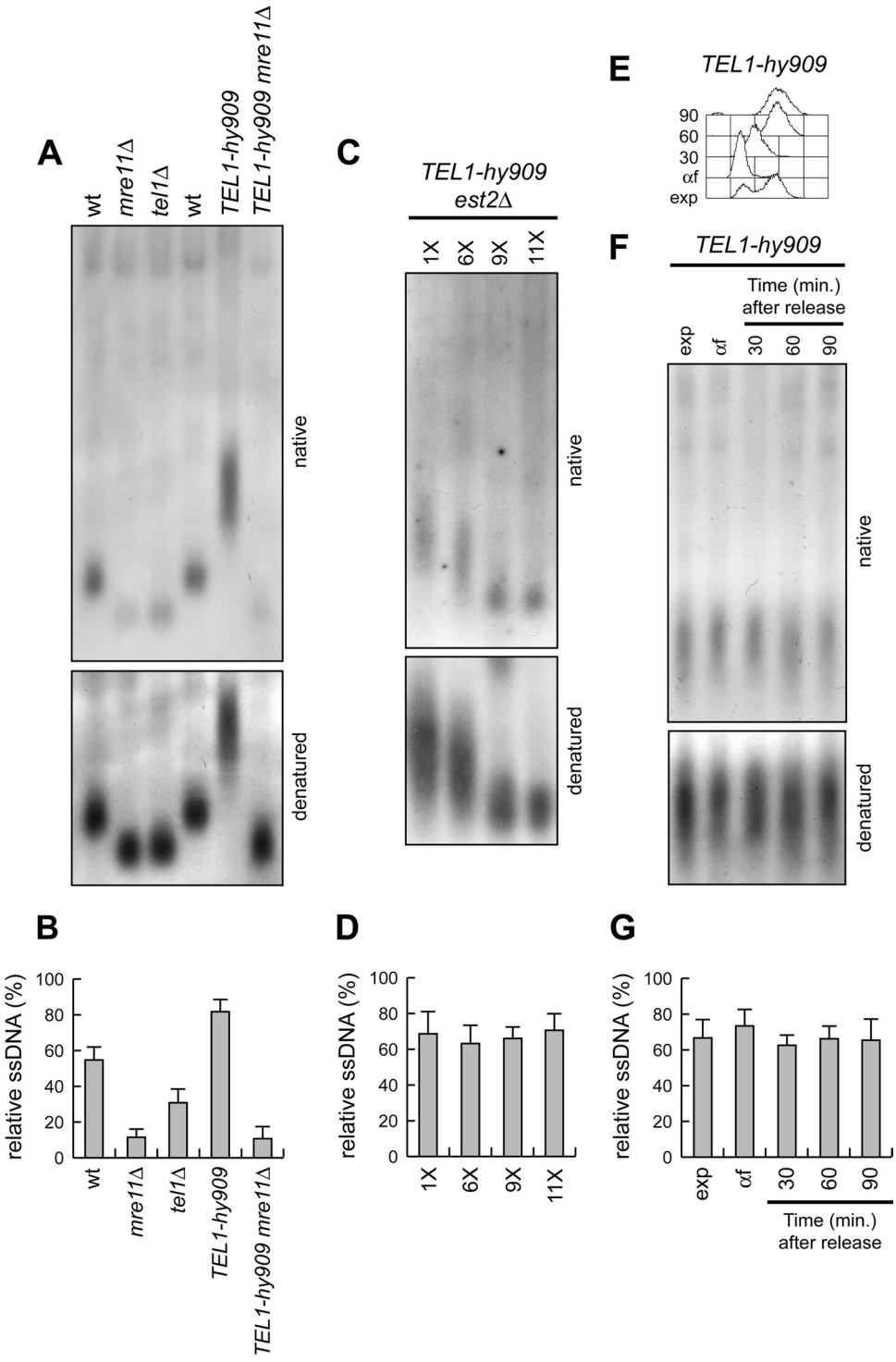

FIG 5 Effects of *tel1*Δ and *TEL1-hy909* alleles on ssDNA formation at native telomeres. (A) Genomic DNA prepared from exponentially growing cells was digested with XhoI, and single-stranded G tails were visualized by in-gel hybridization (native) using an end-labeled C-rich oligonucleotide as a probe. The gel was then denatured and hybridized again with the same probe for loading control (denatured). (B) The amount of native TG-ssDNA, as in panel A, was normalized to the total amount of TG sequences detected in each denatured sample. (C and D) Meiotic tetrads from *EST2*/*est2*Δ *TEL1*/*tel1-hy909* diploid cells were dissected on YEPD plates. (C) After ~25 generations, *TEL1-hy909 est2*Δ spore clones were streaked for successive times (1 to 11 times), and aliquots of cells from the indicated streaks were propagated in YEPD liquid medium for 5 h to prepare genomic DNA for telomeric ssDNA detection, as in panel A. (D) The amount of native TG-ssDNA, as in panel C, was normalized to the total amount of TG sequences detected in each denatured sample. (E to G) Exponentially growing (exp) *TEL1-hy909* cells were arrested in G_1 with α-factor (αf) and released into the cell cycle. (E) Fluorescence-activated cell sorter analysis of DNA content. (F) Genomic DNA prepared at the indicated time points after release from the α-factor block was analyzed for telomeric ssDNA detection, as in panel A. (G) The amount of native TG-ssDNA, as in panel F, was normalized to the total amount of TG sequences detected in each denatured sample. Plotted values in panels B, D, and G are means ± SDs from three independent experiments.

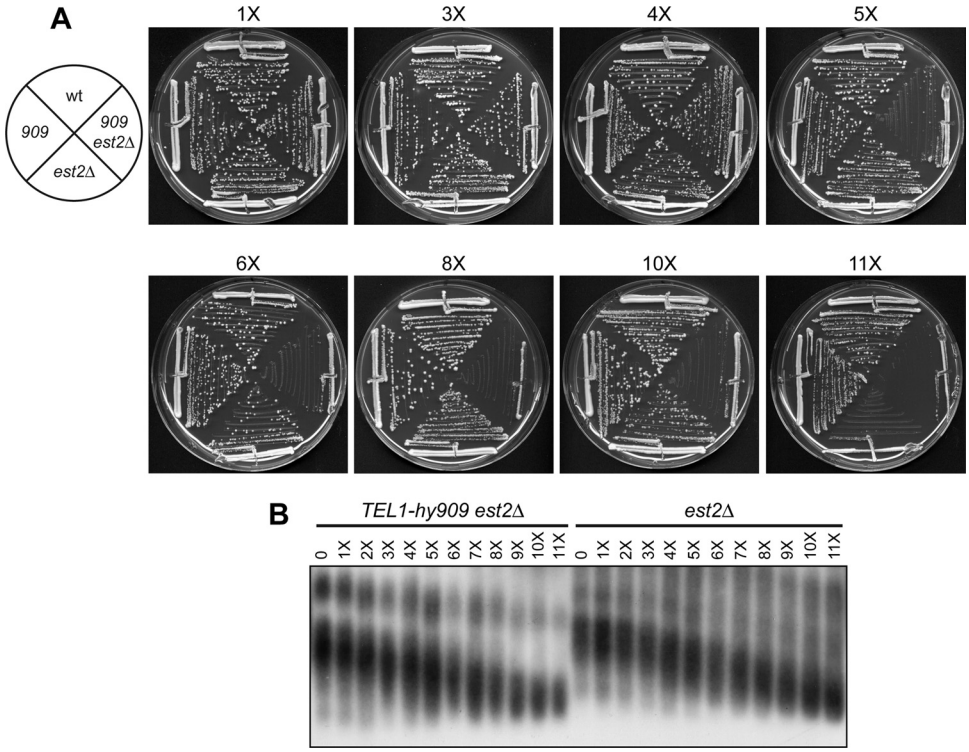

FIG 6 The *TEL1-hy909* mutation accelerates the onset of senescence in *est2*Δ cells. Meiotic tetrads from an *EST2*/*est2*Δ *TEL1*/*tel1-hy909* diploid strain were dissected on YEPD plates. (A) After ~25 generations, spore clones from 15 tetrads were streaked for successive times (1 to 11 times). (B) An aliquot of cells from the indicated streaks was propagated in YEPD liquid medium for 5 h to prepare genomic DNA for telomere length determination by Southern blot analysis. All tetratype tetrads behaved as the one shown in panel A.

the fifth passage, whereas *est2*Δ cells lost viability only at the 11th subculturing (Fig. 6A), indicating that Tel1-hy909 accelerates the onset of senescence in telomerase-negative cells. If ssDNA is the primary signal triggering senescence, as proposed (1), these data suggest that the increased amount of ssDNA in *TEL1-hy909 est2*Δ compared to *est2*Δ cells might explain the accelerated senescence phenotype of the *TEL1-hy909 est2*Δ cells.

***TEL1-hy909* telomeres escape Rif2-mediated inhibition of nucleolytic processing and elongation.** Rif2 inhibits MRX-dependent ssDNA generation at telomeres during both G_1 and G_2 cell cycle phases (6, 7). Since Rif2 has been proposed to compete with Tel1 for binding to MRX (26), the Tel1-hy909 variant might bypass the Rif2-mediated negative regulation of MRX activity. To address this possibility, we compared resection of the DSB adjacent to telomeric repeats in *TEL1-hy909*, *rif2*Δ, and *rif2*Δ *TEL1-hy909* cells. We found that the 5′ C strand at the TG side of the HO cut was degraded with very similar kinetics in G_1-arrested *TEL1-hy909*, *rif2*Δ, and *rif2*Δ *TEL1-hy909* cells (Fig. 7A and B). Similar results were also obtained when degradation of the 5′ C strand was analyzed in the same strains arrested in G_2 (data not shown). Thus, nucleolytic degradation at *TEL1-hy909* telomeres is not sensitive to the inhibitory activity of Rif2, indicating that the increased resection of *TEL1-hy909* telomeres likely reflects failure of Rif2 to negatively regulate their processing.

As Rif2 inhibits telomerase-dependent telomere elongation (29, 52), we investigated whether Tel1-hy909 also overcomes this Rif2-mediated negative regulation of telomere length. We first used the system described in Fig. 2A to analyze the effect of a lack of Rif2 on the kinetics of telomere addition at the DSB end carrying TG sequences in *TEL1-hy909* cells. As a control, we also analyzed the same process in otherwise isogenic *TEL1-hy909* cells lacking Rif1, which negatively regulates telomere length by acting in a pathway different from that involving Rif2 (29, 52). When the HO cut was induced in exponentially growing cells, *rif2*Δ cells elongated the TG DSB end more efficiently than wild-type cells under the same conditions (Fig. 7C), as expected. Sequence addition to this DSB side was also enhanced in *TEL1-hy909* cells (Fig. 7C), indicating that the Tel1-hy909 variant also increases the efficiency of telomere elongation in this assay. Interestingly, telomere addition took place with very similar efficiency in *TEL1-hy909 rif2*Δ double mutant cells and in *rif2*Δ or *TEL1-hy909* single mutants (Fig. 7C), indicating that *TEL1-hy909* telomere length escapes the Rif2-dependent negative control. Differently from Rif2, Rif1 still acts as a negative regulator of telomere length in *TEL1-hy909* cells. In fact, sequence addition to the telomeric DSB side was enhanced in *TEL1-hy909 rif1*Δ double mutant cells compared to both *TEL1-hy909* and *rif1*Δ single mutants (Fig. 7D), although *RIF1* deletion had a more modest effect than *RIF2* deletion in allowing telomere addition (Fig. 7D) (26, 37).

We then analyzed the epistatic relationships between *TEL1-hy909*, *rif2*Δ, and *rif1*Δ alleles in the control of native telomere length. Diploid strains heterozygous for *TEL1-hy909* and either *rif1*Δ or *rif2*Δ were sporulated, and the resulting tetrads were dissected. Because mutations affecting telomere length often exhibit a phenotypic lag, we examined telomere lengths by Southern blot analysis of genomic DNA prepared from subcultures of the hap-

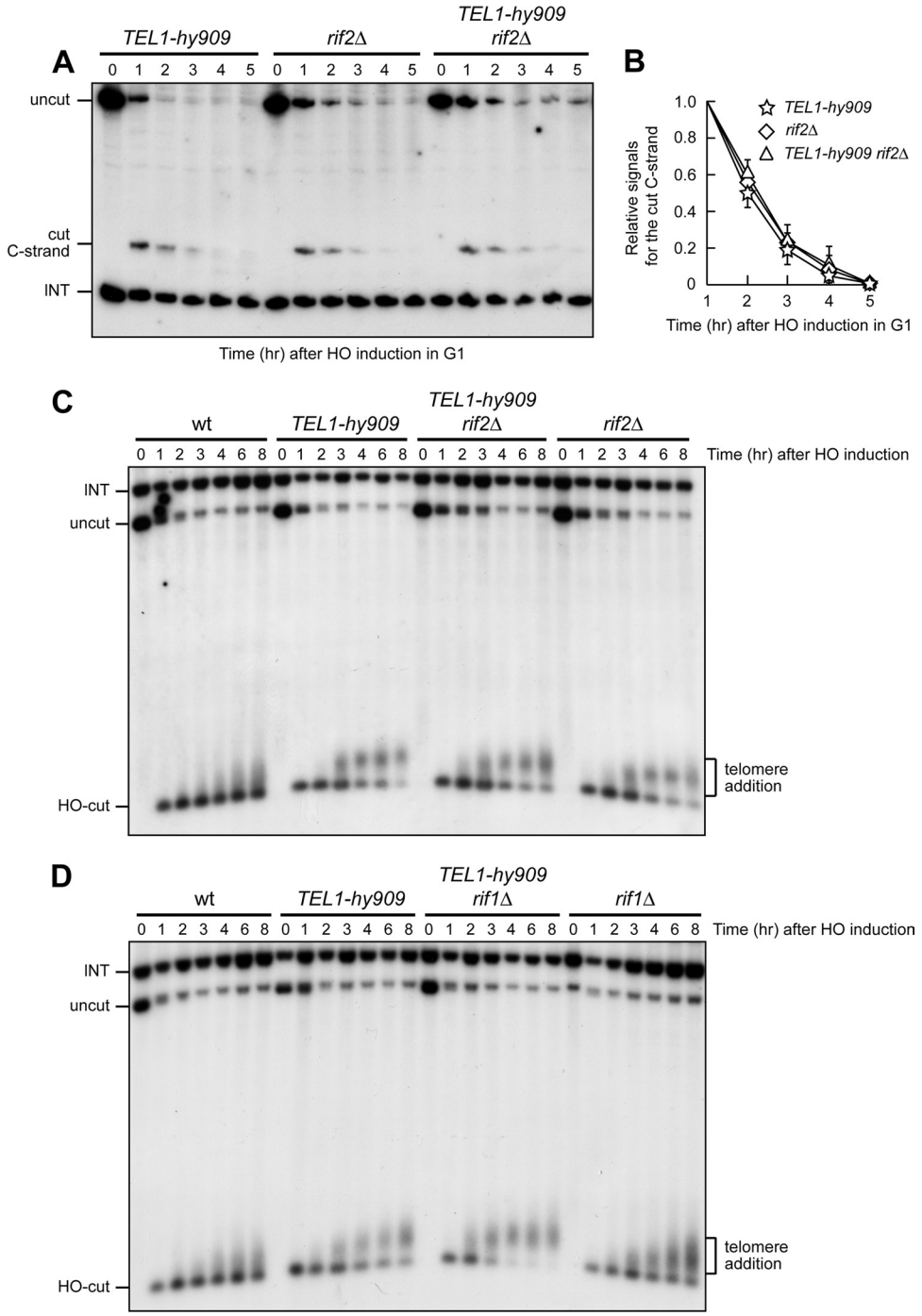

FIG 7 Processing and elongation of a DSB end carrying TG tracts in *TEL1-hy909* cells are not affected by *RIF2* deletion. (A and B) HO expression was induced at time zero by galactose addition to α-factor-arrested cells, all carrying the system described in Fig. 2A. Cells were kept arrested in G_1, and cell cycle arrest was verified by fluorescence-activated cell sorter analysis (data not shown). (A) RsaI- and EcoRV-digested genomic DNA was analyzed as described in the legend to Fig. 2C. (B) Densitometric analysis. Plotted values are means ± SDs from three independent experiments, as in panel A. (C and D) HO expression was induced at time zero by galactose addition to exponentially growing cells. AvaI- and NdeI-digested genomic DNA was subjected to Southern blot analysis using a *TRP1* probe, which reveals the ~800-bp AvaI-HO fragment exposing the TG repeats, whose length progressively increases as new telomere repeats are added. A bracket points out new telomere repeats added to the exposed TG-HO sequence.

loid clones derived from the spores. Telomeres of *TEL1-hy909 rif1*Δ double mutant cells were longer than those of both *TEL1-hy909* and *rif1*Δ single mutants (Fig. 8), whereas *RIF2* deletion did not cause further telomere lengthening in *TEL1-hy909* cells (Fig. 8). Thus, while Rif1 still negatively controls the length of native telomeres in *TEL1-hy909* cells, the same cells also escape the Rif2-mediated negative regulation at native telomeres. Interestingly, *TEL1-hy909* cells had longer telomeres than *rif2*Δ cells (Fig. 8),

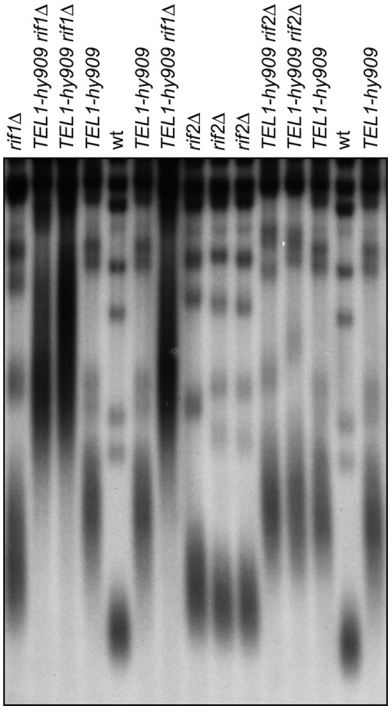

FIG 8 Different effects of *RIF1* and *RIF2* deletion on the length of native *TEL1-hy909* telomeres. XhoI-cut genomic DNA from exponentially growing cell cultures with the indicated genotypes was analyzed as described in the legend to Fig. 1.

indicating that *TEL1-hy909* telomere overelongation cannot be solely attributed to the lack of Rif2-mediated inhibition of telomerase.

Tel1-hy909 is more robustly associated than wild-type Tel1 to DSB ends carrying telomeric repeat sequences. Rif2 is thought to inhibit telomere elongation by counteracting Tel1 association to telomeric DNA (26). Thus, one possibility is that Rif2 is unable to inhibit telomere processing and elongation in *TEL1-hy909* cells because Tel1-hy909 is more robustly associated to the telomeric ends than wild-type Tel1. To investigate this hypothesis, we analyzed by ChIP experiments the binding of HA-tagged Tel1 and Tel1-hy909 variants at the telomeric (TG-HO) and nontelomeric (HO) sides of the HO-induced DSB depicted in Fig. 9A. The HO cut was induced by galactose addition in G_1- or G_2-arrested *TEL1-HA* and *TEL1-hy909-HA* cell cultures that were kept arrested in G_1 (Fig. 9B) or in G_2 (Fig. 9E), respectively. Consistent with the notion that Tel1 association at telomeres is inhibited by Rif2 (26), the amount of wild-type Tel1-HA bound at the TG-HO side of the break was greatly reduced compared to that associated to the nontelomeric (HO) side during both G_1 (Fig. 9C and D) and G_2 (Fig. 9F and G) arrest. Interestingly, the amount of Tel1-hy909-HA bound at the TG-HO DSB end was dramatically higher than that of wild-type Tel1-HA in both G_1 and G_2 (Fig. 9C and F), indicating that Tel1-hy909 is more robustly associated than wild-type Tel1 to DNA ends carrying telomeric DNA. In contrast, the amount of Tel1-hy909-HA that associated to the HO end with no telomeric repeats was similar to that of wild-type Tel1-HA in G_1 cells (Fig. 9D), whereas it was slightly increased in G_2 cells (Fig. 9G), in agreement with the observation that Tel1-hy909 can enhance resection of a nontelomeric DSB end in G_2, but not in G_1.

Tel1-hy909 increases MRX and Est1 persistence at DSB ends carrying telomeric repeats. If Tel1 promotes MRX activity by facilitating MRX persistence onto DNA ends, then the more robust association to telomeric ends of Tel1-hy909 than wild-type Tel1 might lead to increased MRX binding at these ends, thus eventually leading to enhanced telomere resection. We therefore also analyzed G_1- or G_2-arrested wild-type and *TEL1-hy909* cells for the binding of MYC-tagged Mre11 to either the TG-HO telomeric end or the HO nontelomeric end of the HO-induced DSB depicted in Fig. 9A. The association of Mre11 to the TG-HO DSB end was greatly increased in both G_1- and G_2-arrested *TEL1-hy909* cells compared to wild type (Fig. 10A and B). In contrast, Mre11 binding to the nontelomeric DSB end was similar in G_1-arrested wild-type and *TEL1-hy909* cells (Fig. 10C), whereas it was slightly increased in *TEL1-hy909* G_2 cells (Fig. 10D), consistent with the finding that the enhanced resection of DSB ends with no TG sequences in *TEL1-hy909* cells is restricted to the G_2 cell cycle phase (3).

As Tel1 is thought to regulate telomere length by promoting telomerase recruitment at telomeres, increased association of Tel1-hy909 at telomeric ends might also enhance telomerase association to the same ends. Indeed, the amount of MYC-tagged Est1 bound to the TG-HO side of the HO-induced DSB was much higher in G_2-arrested *TEL1-hy909* cells than in wild type (Fig. 10E), suggesting that enhanced Est1 association at *TEL1-hy909* telomeres may account for their overelongation.

DISCUSSION

The MRX complex is required for the recruitment of Tel1 to DSB ends (39). On the other hand, the lack of Tel1 causes a decrease of MRX binding at telomeres (26), suggesting that Tel1 exerts a positive-feedback loop on MRX. However, the physiological relevance of this control was unknown. By studying the effects on telomere processing and elongation of the lack of Tel1 compared with the effects of the dominant Tel1-hy909 variant, we provide evidence that Tel1 is crucial for counteracting Rif2-dependent negative regulation of telomere resection and elongation.

We show that the lack of Tel1, which is known to cause telomere shortening (22), decreases both MRX-dependent resection at a DSB end carrying telomeric repeats and the amount of ssDNA formation at native telomeres. Together with the notion that MRX association at telomeres is impaired by the lack of Tel1 (26), these data indicate that Tel1, once loaded onto DNA ends by MRX, regulates 5′-3′ nucleolytic degradation of telomere ends by promoting MRX activity. This role of Tel1 is not restricted to telomere ends, as the lack of Tel1 was shown to slightly impair generation of ssDNA also at intrachromosomal DSBs (34).

Consistent with a role of Tel1 in regulating telomere end resection, the *TEL1-hy909* mutation, which causes telomerase-dependent telomere overelongation, increases the amount of ssDNA at telomeres. This increase becomes apparent even in the absence of telomerase, indicating that it is due to an enhanced resection rather than to telomerase action. Moreover, the *TEL1-hy909* mutation accelerates the onset of senescence of telomerase-negative cells. As telomeric ssDNA has been proposed to trigger senescence (1), this finding further supports the hypothesis that the Tel1-hy909 variant enhances nucleolytic degradation at telomeres. Accordingly, the lack of Tel1, which reduces the amount of telomeric ssDNA, attenuates the senescence phenotype of telomerase-negative cells (19, 42).

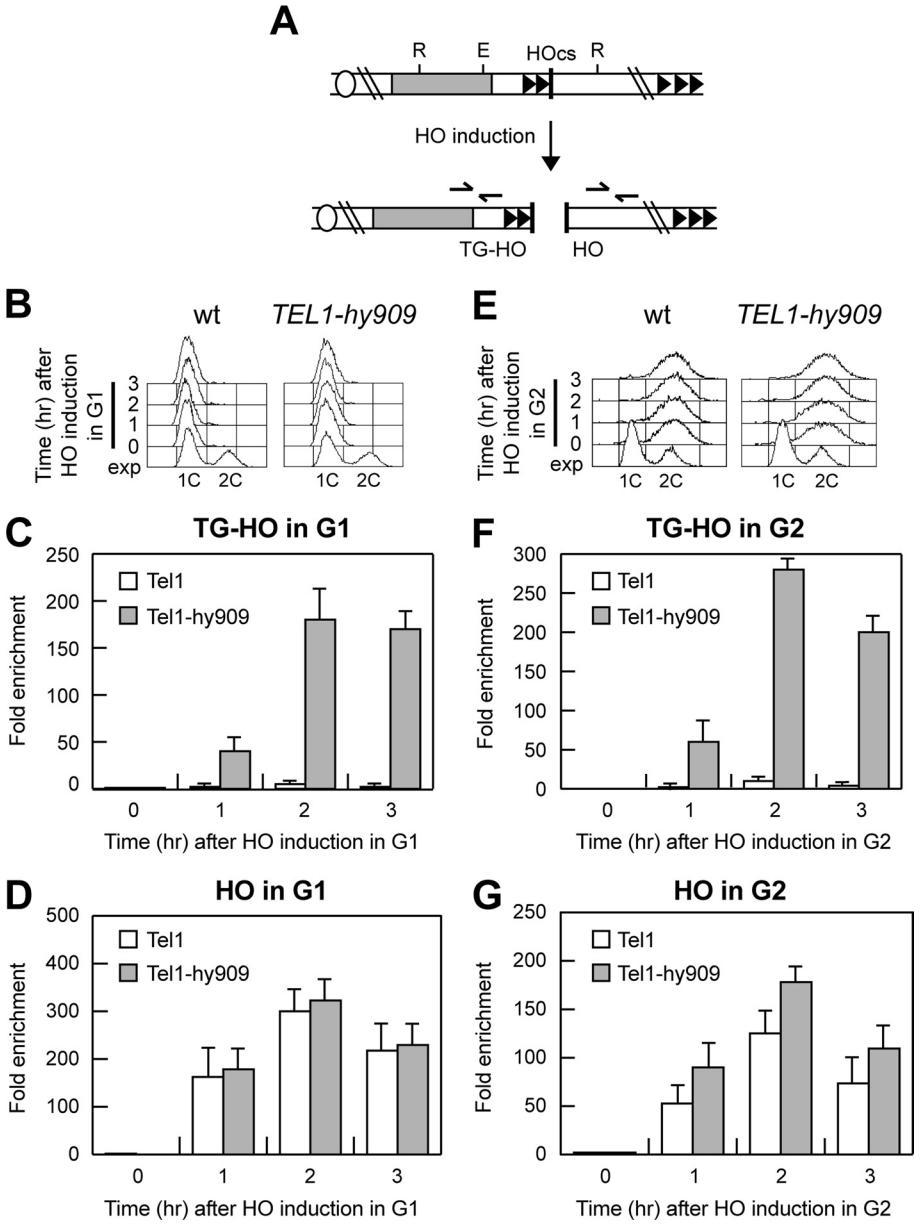

FIG 9 Association of Tel1-HA and Tel1-hy909-HA to DNA ends. (A) The system described in Fig. 2A was used to generate TG-HO and HO DNA ends, and the primers used to detect protein association centromere proximal (TG-HO) or centromere distal (HO) to the HO-induced DSB are represented by arrows in the bottom part of the panel. (B to G) HO expression was induced at time zero by galactose addition to G_1-arrested (B to D) or G_2-arrested (E to G) *TEL1-HA* (wild-type) and *TEL1-hy909-HA* (*TEL1-hy909*) cells, which were kept arrested in G_1 or G_2 by α-factor and nocodazole, respectively. (B and E) Fluorescence-activated cell sorter analysis of DNA content. (C to G) Chromatin samples taken at the indicated times after HO induction were immunoprecipitated with anti-HA antibody. (C and F) Coimmunoprecipitated DNA was analyzed by qPCR using primer pairs located 640 bp centromere proximal to the HO cleavage site (HOcs; TG-HO) and at the nontelomeric *ARO1* fragment of chromosome IV (CON). (D and G) Coimmunoprecipitated DNA was analyzed by qPCR using primer pairs located 550 bp centromere distal to the HO cleavage site (HOcs; HO) and at the nontelomeric *ARO1* fragment of chromosome IV (CON). In all graphs, data are expressed as relative fold enrichment of the TG-HO or HO signal over the CON signal after normalization to input signals for each primer set. The data presented are means ± SDs from three different experiments.

How does Tel1-hy909 enhance telomere processing and elongation? Both the enhanced resection and elongation of *TEL1-hy909* telomeres require Tel1-hy909 kinase activity, further confirming that Tel1 acts as a kinase at telomeres (33). Like most of the other Tel1-hy variants that we found by virtue of their ability to suppress the hypersensitivity to genotoxic agents of *mec1*Δ cells, the Tel1-hy909 variant has enhanced kinase activity *in vitro* compared to wild-type Tel1 (3). However, only the Tel1-hy909 variant confers a striking telomere overelongation phenotype (3), implying that this phenotype cannot be entirely ascribed to the high Tel1-hy909 kinase activity.

Tel1-hy909 is more robustly associated than wild-type Tel1 to DSB ends carrying telomeric repeats during both the G_1 and G_2 cell cycle phases, likely leading to increased MRX and Est1 persis-

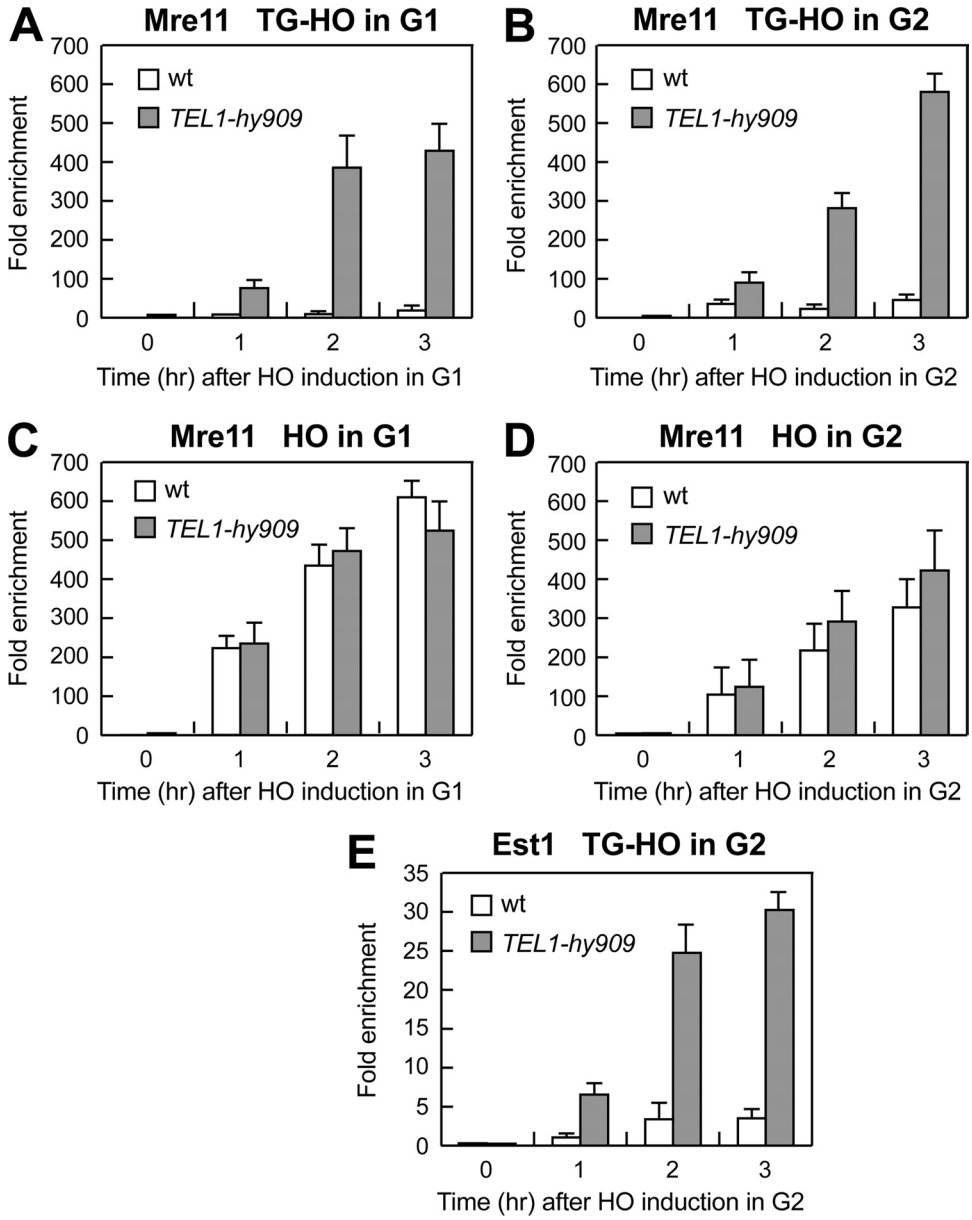

FIG 10 Mre11 and Est1 association to DNA ends in wild-type and *TEL1-hy909* cells. G_1- or G_2-arrested wild-type and *TEL1-hy909* cells carrying the TG-HO system described in Fig. 2A and expressing fully functional MYC-tagged Mre11 (A to D) or MYC-tagged Est1 (E) were treated as described in the legend to Fig. 9, and cell cycle arrest was verified by fluorescence-activated cell sorter analysis (data not shown). Chromatin samples taken at the indicated times after HO induction were immunoprecipitated with anti-MYC antibody. (A, B, and E) Coimmunoprecipitated DNA was analyzed by qPCR with the primer pairs used for Fig. 9C and F. (C and D) Coimmunoprecipitated DNA was analyzed by qPCR with the primer pairs used for Fig. 9D and G. In all graphs, data are expressed as relative fold enrichment of the TG-HO or HO signal over the CON signal after normalization to input signals for each primer set. The data presented are means ± SDs from three different experiments.

tence at telomeric ends. In fact, the amounts of Mre11 and Est1 bound to telomeric DNA ends are higher in *TEL1-hy909* cells than wild-type cells. While enhanced MRX association could explain the increased efficiency of *TEL1-hy909* telomere resection, stabilization of Est1 binding to telomeric ends may account for the overelongation of *TEL1-hy909* telomeres. Because MRX is required to load Tel1 onto DNA ends (39) and to support Tel1-hy909 activities, this robust Tel1-hy909 association to telomeres may be due to an increased ability of Tel1-hy909 to interact with MRX compared to wild-type Tel1, as also suggested by the dominant effects of the *TEL1-hy909* allele. Unfortunately, we have so far been unable to coimmunoprecipitate Tel1 with MRX to assess this possibility.

MRX-dependent generation of ssDNA at telomeres is prevented by Rif2 during both G_1 and G_2 (7). We show that neither processing nor elongation of *TEL1-hy909* telomeres is inhibited by Rif2, indicating a failure of Rif2 to counteract MRX activity in the presence of the Tel1-hy909 variant. As Rif2 has been proposed to compete with Tel1 for binding to MRX (26), the dominant Tel1-hy909 variant might escape the Rif2-mediated negative con-

trol by binding to MRX more efficiently than wild-type Tel1. Because Tel1 exerts a positive-feedback loop on MRX, this robust Tel1-hy909 recruitment may in turn stabilize MRX association to telomeric ends, possibly through phosphorylation events.

The action of Tel1-hy909 is not restricted to telomeric ends, as Tel1-hy909 also enhances resection at intrachromosomal DSBs (3). However, this Tel1-hy909 function is restricted to the G_2 cell cycle phase, because Tel1-hy909 is not able to enhance resection in G_1 (when Cdk1 activity is low) of a DSB end without telomeric sequences, while it does it when the DSB end carries TG repeats. Noteworthy, while Rif2 prevents MRX activity specifically at telomeres, MRX-dependent resection at DSBs devoid of telomeric repeats is counteracted by Yku, which exerts this inhibitory role only in G_1 (11). These observations, together with our finding that Tel1 regulates telomere resection by promoting MRX function, suggest that Tel1-hy909 is unable to promote resection in G_1 at DSB ends without telomeric repeats because it cannot overcome the inhibitory effect exerted by Yku on MRX. This inability does not prevent Tel1-hy909 from enhancing MRX-dependent resection at telomeres, because Yku was shown to protect them mainly from Exo1 and not from MRX (7, 48). Since Yku-mediated inhibition of MRX activity at intrachromosomal DSBs is relieved in G_2 (11), Tel1-hy909 can promote resection of intrachromosomal DSBs only during this cell cycle stage. Consistent with different mechanisms inhibiting MRX activity at telomeres than at DSBs, MRX-dependent resection in G_1 is completely abolished at a DSB end with TG repeats, whereas it takes place, although less efficiently than in G_2, when the DSB is devoid of telomeric sequences. Interestingly, the resection kinetics of DSB ends with no TG repeats in G_1-arrested wild-type cells is similar to that occurring in G_1-arrested *TEL1-hy909* cells when the DSB end carries TG tracts (compare Fig. 3 and 4). Furthermore, the amount of MRX bound to DSB ends with no telomeric sequences in wild-type cells is similar to the MRX amount that is recruited at DSB ends carrying TG repeats in *TEL1-hy909* cells. Thus, the difference in terms of ssDNA generation at DSBs versus telomeric DNA ends appears to rely on Rif2-mediated inhibition of Tel1 and, hence, of MRX activity.

The molecular mechanism underlying Tel1-mediated regulation of telomere length has not yet been solved. The finding that the amount of telomeric G tails is reduced by the lack of Tel1, whereas it is increased in *TEL1-hy909* cells, leads to a model, also suggested by Lundblad and colleagues (19), where Tel1 function in telomere length maintenance can be linked to its role in generating telomeric G tails, which are the substrates of telomerase. In this model, the telomere length defect observed in *tel1*Δ cells might be a consequence of the reduced ssDNA amount at the telomeric ends, whereas the increased ssDNA generation at *TEL1-hy909* telomeres might improve telomerase-dependent elongation by increasing the substrates available for the telomerase enzyme. However, the finding that the single-stranded G-tail signal was lower in *mre11*Δ cells than in *tel1*Δ cells, which display a similar telomere length defect and are likely defective in the same telomere length maintenance pathway (41), is inconsistent with the idea that Tel1 function in telomere length maintenance is limited to ssDNA generation.

The correlation between telomere overelongation and increased Est1 binding at *TEL1-hy909* telomeres provides additional support for a model in which Tel1 is a positive activator of telomerase. Because the kinase activity of Tel1 is needed for its role in telomere maintenance (33), phosphorylation of one or more telomere binding proteins by Tel1 could increase the frequency of elongation by making the telomeric chromatin more accessible to telomerase. In this scenario, the robust association of hyperactive Tel1-hy909 kinase at telomeres may improve the efficiency of this process.

In conclusion, regulation of telomere processing and elongation appears to rely on a balance between Tel1 and Rif2 activities. As Tel1 hyperactivation can improve both telomere resection and telomerase action, Rif2-dependent inhibition of Tel1/MRX function at telomeres is important to ensure the maintenance of telomere identity by limiting ssDNA generation and elongation. In contrast, such a control appears to be dispensable at intrachromosomal DSBs, where generation of ssDNA is necessary to repair the break.

ACKNOWLEDGMENTS

We thank D. Gottschling, J. Haber, T. Petes, D. Shore, K. Sugimoto, and T. Weinert for yeast strains. We thank Laura Candelora for the help in some experiments.

This work was supported by grants from the Associazione Italiana per la Ricerca sul Cancro (grant number IG11407), Cofinanziamento 2008 MIUR/Università di Milano-Bicocca to M.P.L., and Cofinanziamento 2009 MIUR/Università di Milano-Bicocca to G.L. M.M. was supported by a fellowship from the Fondazione Confalonieri.

REFERENCES

1. **Abdallah P, et al.** 2009. A two-step model for senescence triggered by a single critically short telomere. Nat. Cell Biol. **11**:988–993.
2. **Arnerić M, Lingner J.** 2007. Tel1 kinase and subtelomere-bound Tbf1 mediate preferential elongation of short telomeres by telomerase in yeast. EMBO Rep. **8**:1080–1085.
3. **Baldo V, Testoni V, Lucchini G, Longhese MP.** 2008. Dominant *TEL1-hy* mutations compensate for Mec1 lack of functions in the DNA damage response. Mol. Cell. Biol. **28**:358–375.
4. **Bianchi A, Shore D.** 2007. Increased association of telomerase with short telomeres in yeast. Genes Dev. **21**:1726–1730.
5. **Bianchi A, Negrini S, Shore D.** 2004. Delivery of yeast telomerase to a DNA break depends on the recruitment functions of Cdc13 and Est1. Mol. Cell **16**:139–146.
6. **Bonetti D, Clerici M, Manfrini N, Lucchini G, Longhese MP.** 2010. The MRX complex plays multiple functions in resection of Yku- and Rif2-protected DNA ends. PLoS One **5**:e14142.
7. **Bonetti D, et al.** 2010. Shelterin-like proteins and Yku inhibit nucleolytic processing of *Saccharomyces cerevisiae* telomeres. PLoS Genet. **6**:e1000966.
8. **Bonetti D, Martina M, Clerici M, Lucchini G, Longhese MP.** 2009. Multiple pathways regulate 3′ overhang generation at *S. cerevisiae* telomeres. Mol. Cell **35**:70–81.
9. **Chan A, Boulé JB, Zakian VA.** 2008. Two pathways recruit telomerase to *Saccharomyces cerevisiae* telomeres. PLoS Genet. **4**:e1000236.
10. **Chang M, Arneric M, Lingner J.** 2007. Telomerase repeat addition processivity is increased at critically short telomeres in a Tel1-dependent manner in *Saccharomyces cerevisiae*. Genes Dev. **21**:2485–2494.
11. **Clerici M, Mantiero D, Guerini I, Lucchini G, Longhese MP.** 2008. The Yku70-Yku80 complex contributes to regulate double-strand break processing and checkpoint activation during the cell cycle. EMBO Rep. **9**:810–818.
12. **Conrad MN, Wright JH, Wolf AJ, Zakian VA.** 1990. RAP1 protein interacts with yeast telomeres in vivo: overproduction alters telomere structure and decreases chromosome stability. Cell **63**:739–750.
13. **Diede SJ, Gottschling DE.** 1999. Telomerase-mediated telomere addition in vivo requires DNA primase and DNA polymerases α and δ. Cell **99**:723–733.
14. **Diede SJ, Gottschling DE.** 2001. Exonuclease activity is required for sequence addition and Cdc13p loading at a de novo telomere. Curr. Biol. **11**:1336–1340.
15. **Dionne I, Wellinger RJ.** 1996. Cell cycle-regulated generation of single-

stranded G-rich DNA in the absence of telomerase. Proc. Natl. Acad. Sci. U. S. A. **93**:13902–13907.
16. **Evans SK, Lundblad V.** 1999. Est1 and Cdc13 as comediators of telomerase access. Science **286**:117–120.
17. **Frank CJ, Hyde M, Greider CW.** 2006. Regulation of telomere elongation by the cyclin-dependent kinase CDK1. Mol. Cell **24**:423–432.
18. **Gallardo F, et al.** 2011. Live cell imaging of telomerase RNA dynamics reveals cell cycle-dependent clustering of telomerase at elongating telomeres. Mol. Cell **44**:819–827.
19. **Gao H, et al.** 2010. Telomerase recruitment in *Saccharomyces cerevisiae* is not dependent on Tel1-mediated phosphorylation of Cdc13. Genetics **186**:1147–1159.
20. **Gomes NM, Shay JW, Wright WE.** 2010. Telomere biology in Metazoa. FEBS Lett. **584**:3741–3751.
21. **Goudsouzian LK, Tuzon CT, Zakian VA.** 2006. *S. cerevisiae* Tel1p and Mre11p are required for normal levels of Est1p and Est2p telomere association. Mol. Cell **24**:603–610.
22. **Greenwell PW, et al.** 1995. *TEL1*, a gene involved in controlling telomere length in *S. cerevisiae*, is homologous to the human ataxia telangiectasia gene. Cell **82**:823–829.
23. **Greider CW, Blackburn EH.** 1985. Identification of a specific telomere terminal transferase activity in *Tetrahymena* extracts. Cell **43**:405–413.
24. **Hardy CF, Sussel L, Shore D.** 1992. A RAP1-interacting protein involved in transcriptional silencing and telomere length regulation. Genes Dev. **6**:801–814.
25. **Hector RE, et al.** 2007. Tel1p preferentially associates with short telomeres to stimulate their elongation. Mol. Cell **27**:851–858.
26. **Hirano Y, Fukunaga K, Sugimoto K.** 2009. Rif1 and Rif2 inhibit localization of Tel1 to DNA ends. Mol. Cell **33**:312–322.
27. **Ira G, et al.** 2004. DNA end resection, homologous recombination and DNA damage checkpoint activation require CDK1. Nature **431**:1011–1017.
28. **Larrivée M, LeBel C, Wellinger RJ.** 2004. The generation of proper constitutive G-tails on yeast telomeres is dependent on the MRX complex. Genes Dev. **18**:1391–1396.
29. **Levy DL, Blackburn EH.** 2004. Counting of Rif1p and Rif2p on *Saccharomyces cerevisiae* telomeres regulates telomere length. Mol. Cell. Biol. **24**:10857–10867.
30. **Longhese MP.** 2008. DNA damage response at functional and dysfunctional telomeres. Genes Dev. **22**:125–140.
31. **Longhese MP, Bonetti D, Manfrini N, Clerici M.** 2010. Mechanisms and regulation of DNA end resection. EMBO J. **29**:2864–2874.
32. **Makarov VL, Hirose Y, Langmore JP.** 1997. Long G tails at both ends of human chromosomes suggest a C-strand degradation mechanism for telomere shortening. Cell **88**:657–666.
33. **Mallory JC, Petes TD.** 2000. Protein kinase activity of Tel1p and Mec1p, two *Saccharomyces cerevisiae* proteins related to the human ATM protein kinase. Proc. Natl. Acad. Sci. U. S. A. **97**:13749–13754.
34. **Mantiero D, Clerici M, Lucchini G, Longhese MP.** 2007. Dual role for *Saccharomyces cerevisiae* Tel1 in the checkpoint response to double-strand breaks. EMBO Rep. **8**:380–387.
35. **Marcand S, Brevet V, Gilson E.** 1999. Progressive cis-inhibition of telomerase upon telomere elongation. EMBO J. **18**:3509–3519.
36. **Marcand S, Brevet V, Mann C, Gilson E.** 2000. Cell cycle restriction of telomere elongation. Curr. Biol. **10**:487–490.
37. **McGee JS, et al.** 2010. Reduced Rif2 and lack of Mec1 target short telomeres for elongation rather than double-strand break repair. Nat. Struct. Mol. Biol. **17**:1438–1445.
38. **Michelson RJ, Rosenstein S, Weinert T.** 2005. A telomeric repeat sequence adjacent to a DNA double-stranded break produces an anticheckpoint. Genes Dev. **19**:2546–2559.
39. **Nakada D, Matsumoto K, Sugimoto K.** 2003. ATM-related Tel1 associates with double-strand breaks through an Xrs2-dependent mechanism. Genes Dev. **17**:1957–1962.
40. **Pennock E, Buckley K, Lundblad V.** 2001. Cdc13 delivers separate complexes to the telomere for end protection and replication. Cell **104**:387–396.
41. **Ritchie KB, Petes TD.** 2000. The Mre11p/Rad50p/Xrs2p complex and the Tel1p function in a single pathway for telomere maintenance in yeast. Genetics **155**:475–479.
42. **Ritchie KB, Mallory JC, Petes TD.** 1999. Interactions of *TLC1* (which encodes the RNA subunit of telomerase), *TEL1*, and *MEC1* in regulating telomere length in the yeast *Saccharomyces cerevisiae.* Mol. Cell. Biol. **19**:6065–6075.
43. **Sabourin M, Tuzon CT, Zakian VA.** 2007. Telomerase and Tel1p preferentially associate with short telomeres in *S. cerevisiae.* Mol. Cell **27**:550–561.
44. **Taggart AK, Teng SC, Zakian VA.** 2002. Est1p as a cell cycle-regulated activator of telomere-bound telomerase. Science **297**:1023–1026.
45. **Teixeira MT, Arneric M, Sperisen P, Lingner J.** 2004. Telomere length homeostasis is achieved via a switch between telomerase-extendible and -nonextendible states. Cell **117**:323–335.
46. **Tseng SF, Lin JJ, Teng SC.** 2006. The telomerase-recruitment domain of the telomere binding protein Cdc13 is regulated by Mec1p/Tel1p-dependent phosphorylation. Nucleic Acids Res. **34**:6327–6336.
47. **Viscardi V, Bonetti D, Cartagena-Lirola H, Lucchini G, Longhese MP.** 2007. MRX-dependent DNA damage response to short telomeres. Mol. Biol. Cell **18**:3047–3058.
48. **Vodenicharov MD, Laterreur N, Wellinger RJ.** 2010. Telomere capping in non-dividing yeast cells requires Yku and Rap1. EMBO J. **29**:3007–3019.
49. **Vodenicharov MD, Wellinger RJ.** 2006. DNA degradation at unprotected telomeres in yeast is regulated by the CDK1 (Cdc28/Clb) cell-cycle kinase. Mol. Cell **24**:127–137.
50. **Wellinger RJ, Wolf AJ, Zakian VA.** 1993. *Saccharomyces* telomeres acquire single-strand TG1-3 tails late in S phase. Cell **72**:51–60.
51. **Wellinger RJ, Ethier K, Labrecque P, Zakian VA.** 1996. Evidence for a new step in telomere maintenance. Cell **85**:423–433.
52. **Wotton D, Shore D.** 1997. A novel Rap1p-interacting factor, Rif2p, cooperates with Rif1p to regulate telomere length in *Saccharomyces cerevisiae.* Genes Dev. **11**:748–760.